Transverse polarization transfer $D_{NN}(0°)$ measurements for the (p,n) reaction on ^{58}Ni and ^{90}Zr at $E_p = 80$ MeV

H. Sakai, N. Matsuoka, T. Saito, A. Shimizu, and M. Tosaki
Research Center for Nuclear Physics, Osaka University, Mihogaoka 10-1, Ibaraki, Osaka 567, Japan

M. Ieiri, K. Imai, and A. Sakaguchi*
Department of Physics, Kyoto University, Kitashirakawa, Sakyoku, Kyoto 606, Japan

T. Motobayashi
Department of Physics, Rikkyo University, Nishi-Ikebukuro, Toshima, Tokyo 171, Japan
(Received 12 November 1986)

Transverse polarization transfer coefficients for the (p,n) reaction on ^{58}Ni and ^{90}Zr targets have been measured at $E_p = 80$ MeV and $\theta = 0°$. Observed values for the Gamow-Teller giant resonance region are $D_{NN} = -0.36 \pm 0.07$ and -0.18 ± 0.05 for ^{58}Ni and ^{90}Zr targets, respectively, consistent with predominantly spin-flip transitions. Those for the dipole resonance are $D_{NN} = 0.14 \pm 0.03$ and 0.11 ± 0.03, indicating the coexistence of the spin-flip resonance with a non-spin-flip resonance. Finite positive D_{NN} values are observed up to an excitation energy of 30 MeV on both targets, showing the importance of the single step process. The obtained results are interpreted in terms of a plane-wave impulse approximation. In conjunction with the higher energy D_{NN} data, the transition strength ratios of non-spin-flip to spin-flip, and the D_{NN} values pertinent to spin-flip transitions, have been deduced empirically for the Gamow-Teller resonance, the dipole resonance, and $E_x = 28$ MeV regions in the ^{90}Zr(p,n) reaction.

I. INTRODUCTION

Isovector spin excitation modes in nuclei via the (p,n) reaction at intermediate energies have recently attracted particular interest, partly due to the phenomenon of quenching in the Gamow-Teller (GT) strength.[1] The GT giant resonance appears on a continuum background whose shape and magnitude are not known. Uncertainties in the decomposition of the spectrum into GT resonance and background seriously limit the accuracy in obtaining the GT strength. A lot of experiments as well as theoretical studies have been performed to understand spin excitation modes. It is obviously desirable to study the spin-flip strength as directly as possible by experiment. The transverse polarization transfer D_{NN} may provide such a tool. It has been pointed out by Moss[2] that D_{NN} depends strongly on the transferred spin (ΔS) and orbital angular momentum (ΔL), but depends rather weakly on distortions and on details of nuclear structure.

In this article we report the results of transverse polarization transfer measurements for the ^{58}Ni(p,n) and ^{90}Zr(p,n) reaction at 0° and $E_p = 80$ MeV. The data are interpreted in terms of a plane-wave impulse approximation model. These data provide important information about the spin-flip and non-spin-flip strength distributions. In particular, two quantities, the transition strength ratio of the spin flip over non-spin-flip and the D_{NN} value deduced directly from the present D_{NN} data, are incorporated with higher bombarding energy data, employing the empirically determined energy dependence of spin-flip to non-spin-flip strengths $V_{\sigma\tau}/V_\tau$. It may be worthwhile to note that non-spin-flip transitions should be enhanced at $E_p = 80$ MeV relative to spin-flip transitions compared to higher incident energies due to the strong energy dependence of effective interactions, particularly V_τ. A part of this work has been reported elsewhere.[3]

II. EXPERIMENTAL TECHNIQUE

The AVF cyclotron at the Research Center for Nuclear Physics (RCNP), Osaka University, was used to provide a polarized proton beam of energy 80 MeV. The D_{NN} measurements were carried out at the 0° neutron time-of-flight (ZNTOF) facility[4] at RCNP. The targets were self-supporting metallic foils (99% ^{58}Ni, 209 mg/cm^2; 99% ^{90}Zr, $\sim$110 mg/cm^2). The neutron flight paths were 6 m for the measurement of the ^{58}Ni target and 7 m for that of the ^{90}Zr target. The short flight path and rather thick target led to a reasonable counting rate, but also to some sacrifice in the energy resolution ΔE. Typical values of energy resolution were $\Delta E \simeq 2.1$ MeV for $E_n = 60$ MeV, i.e., GT giant resonance region, and $\Delta E \simeq 1.6$ MeV for $E_n = 50$ MeV, i.e., dipole giant resonance region.

The transverse polarization transfer D_{NN} is given by

$$[1 + p_p A(\theta)] p_n = P(\theta) + p_p D_{NN}(\theta) , \quad (1)$$

where p_p (p_n) is the incident proton (outgoing neutron) polarization, A is the analyzing power, and P is the polarization produced in the reaction. At a scattering angle of 0°, $A = P = 0$, and Eq. (1) becomes

$$p_n = p_p D_{NN}(0°) . \quad (2)$$

Therefore, at 0° the neutron polarization can be completely flipped by flipping the proton polarization. This fact allows us to cancel most false asymmetries caused by misalignment. The D_{NN} is written as K_y^y in the Madison convention.[5] The relation between the transverse spin-flip probability S_{NN} and D_{NN} is $D_{NN}=1-2S_{NN}$.

The proton beam polarization was $|p_p|=0.80$—0.85 and its orientation was reversed every second. Typical beam currents were 20—30 nA.

The neutron polarimeter consisted of five detectors and it utilized the analyzing power of n-p scattering from the hydrogen nuclei in the scatterer. A schematic layout is shown in Fig. 1. The scatterer was a liquid scintillation detector (NE213) 12.7 cm in diameter and 12.7 cm high. Scattered neutrons were detected with two sets (left and right) of side detectors positioned at 30° with respect to the incident neutron axis. Each side detector consisted of two detectors, a cylindrical liquid scintillation detector (NE213) 12.7 cm in diameter and 12.7 cm high, followed by a cylindrical plastic scintillation detector 12.7 cm in diameter and 12.7 cm high. The effective analyzing powers of the polarimeter were empirically calibrated at $E_n=45$, 60, and 75 MeV by using an "analogue relation" method.[6] The analyzing powers were determined by observing neutrons in the reaction of ^{6}Li$(\vec{p},\vec{n})^6$Be (g.s., 0^+) at $\theta=0°$ whose polarizations were deduced from the measured D_{NN} values of the ^{6}Li$(\vec{p},\vec{p}\,')^6$Be* (3.562 MeV, 0^+) reaction. Details of this new calibration method are described in Ref. 6.

III. D_{NN} IN TERMS OF PLANE WAVE IMPULSE APPROXIMATION

To get insight into the physics of transverse polarization transfer, the expressions[2] of D_{NN} in terms of a plane wave impulse approximation (PWIA) will be given. The nucleon-nucleon transition amplitude is given by

$$\bar{M}_\mu(q)=\left\langle \mu \left| \sum_{i=1}^{A} e^{i\mathbf{q}\cdot\mathbf{r}} M(q) \right| 0 \right\rangle , \tag{3}$$

where $\mathbf{q}=\mathbf{k}_p-\mathbf{k}_{p'}$ and $\mathbf{k}_p$ ($\mathbf{k}_{p'}$) is the projectile (ejectile) momentum. μ is the projection of the total angular momentum transfer along the q axis. The $M(q)$ is the free nucleon-nucleon scattering amplitude, which may be written as

$$\begin{aligned} M(q)=&A+B\boldsymbol{\sigma}_i\cdot\hat{\mathbf{n}}\boldsymbol{\sigma}_p\cdot\hat{\mathbf{n}}+C(\boldsymbol{\sigma}_i+\boldsymbol{\sigma}_p)\cdot\hat{\mathbf{n}} \\ &+E\boldsymbol{\sigma}_i\cdot\hat{\mathbf{q}}\boldsymbol{\sigma}_p\cdot\hat{\mathbf{q}}+F\boldsymbol{\sigma}_i\cdot\hat{\mathbf{Q}}\boldsymbol{\sigma}_p\cdot\hat{\mathbf{Q}} , \end{aligned} \tag{4}$$

where i (p) denotes a target (projectile) nucleon and the unit vectors $(\hat{\mathbf{Q}},\hat{\mathbf{n}},\hat{\mathbf{q}})$ are in the $\mathbf{k}_p+\mathbf{k}_{p'}$, $\mathbf{k}_p\times\mathbf{k}_{p'}$, and $\mathbf{k}_p-\mathbf{k}_{p'}$ directions.

The transverse polarization transfer is defined by

$$\sigma_0 D_{ij}=\sum_\mu \mathrm{Tr}(\bar{M}_\mu\sigma_i\bar{M}_\mu^\dagger\sigma_j) , \tag{5}$$

where $\sigma_0=\sum_\mu \mathrm{Tr}(\bar{M}_\mu\bar{M}_\mu^\dagger)$. At 0° the D_{NN} becomes simple due to the fact that $C=0$ and $B=E$. For unnatural parity transitions,

$$\sigma_0 D_{NN}=X_T^2(B^2-F^2)-X_L^2B^2 , \tag{6}$$

where

$$\sigma_0=X_T^2(B^2+F^2)+X_L^2B^2 , \tag{7}$$

and X_T (X_L) is the transverse (longitudinal) form factor given by

$$\begin{aligned} X_T=&\left[\frac{\Delta J+1}{2(2\Delta J-1)}\right]^{1/2} Q_{\Delta J\,\Delta J-1} \\ &+\left[\frac{\Delta J}{2(2\Delta J+3)}\right]^{1/2} Q_{\Delta J\,\Delta J+1} , \\ X_L=&\left[\frac{\Delta J}{2\Delta J-1}\right]^{1/2} Q_{\Delta J\,\Delta J-1} \\ &-\left[\frac{\Delta J+1}{2\Delta J+3}\right]^{1/2} Q_{\Delta J\,\Delta J+1} , \end{aligned} \tag{8}$$

where $Q_{\Delta J\,\Delta L}$ is a reduced matrix element[7] with spin ΔJ and orbital angular momentum ΔL. For natural parity transitions,

$$\sigma_0 D_{NN}=\tfrac{1}{2}Q_{\Delta J\,\Delta L}^2(B^2-F^2)+Q_{\Delta J}^2A^2 , \tag{9}$$

where

$$\sigma_0=\tfrac{1}{2}Q_{\Delta J\,\Delta L}^2(B^2+F^2)+Q_{\Delta J}^2A^2 , \tag{10}$$

and $Q_{\Delta J\,\Delta L}$ ($Q_{\Delta J}$) is the form factor with (without) spin transfer.

If, as if often the case, a transition is dominated by a single ΔL value, Eq. (8) becomes simple. Furthermore, if the interaction is purely central ($B=E=F$), the D_{NN} associated with angular momentum transfers $\Delta L,\Delta S,\Delta J$ becomes[2]

$$D_{NN}(0°)=\begin{cases} +1 \text{ for } \Delta S=0,\ \Delta J=\Delta L , \\ 0 \text{ for } \Delta S=1,\ \Delta J=\Delta L , \\ -\dfrac{\Delta J}{2\Delta J+1} \text{ for } \Delta S=1,\ \Delta J=\Delta L+1 , \\ -\dfrac{\Delta J+1}{2\Delta J+1} \text{ for } \Delta S=1,\ \Delta J=\Delta L-1 . \end{cases} \tag{11}$$

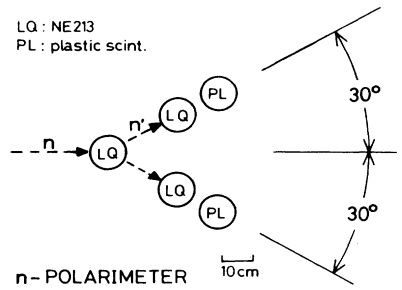

FIG. 1. Schematic arrangement of the neutron polarimeter. The scatterer is the liquid scintillator (LQ) and the side detectors are the LQ and the plastic scintillator (PL). The detectors are all 12.7 cm in diameter and 12.7 cm high.

Thus, for unnatural parity transitions, $D_{NN} \leq -\frac{1}{3}$, and for natural parity transitions, $D_{NN} \geq 0$. The Gamow-Teller transition $\Delta S=1, \Delta J=1$ gives $D_{NN}(0°)=-\frac{1}{3}$. In this paper we will make use of Eq. (11).

A momentum transfer q dependence of D_{NN} has been studied[2,8] and it has been shown that the sensitivity of D_{NN} to unnatural parity transitions is lost at large momentum transfer, $q>1$ fm^{-1}, i.e., at large negative Q value and it becomes $D_{NN}(0°)\simeq 0$. It has also been pointed out[2,8] that the inclusion of distortion, in general, does not alter the D_{NN} value at small momentum transfer, $q \leq 0.5$ fm^{-1}.

IV. RESULTS

Spectra for the ^{58}Ni (p,n) and ^{90}Zr(p,n) reactions are shown in Figs. 2 and 3, respectively. The upper part of the figures shows the double differential cross section and the lower part is the transverse polarization transfer D_{NN} for 1-MeV energy bins. The D_{NN} is extracted without any background subtraction.

Gross features observed for both targets are quite similar to each other. The Gamow-Teller (GT) giant resonance peak is not so prominent at this projectile energy; instead, the dipole resonance peak dominates the energy spectrum. These energy spectra are consistent with those observed at higher projectile energies[9,10] at a similar momentum transfer. For example, the energy spectrum for the ^{58}Ni(p,n) reaction at 5° and $E_p=120$ MeV reported by Rapaport *et al.*,[9] which has almost the same momentum transfer ($q\simeq 0.18$ fm^{-1}) for the GT resonance region, resembles the present data if the effect due to the present poor energy resolution is taken into account.

The observed D_{NN} values also show expected features. The D_{NN} values around the 0^+ ($\Delta L=0$, $\Delta S=0$) isobaric analog state (IAS) transition are positive (0.4—0.5), as expected for $D_{NN}(\text{IAS})=+1$; those around the GT transition region are negative, indicating the dominance of

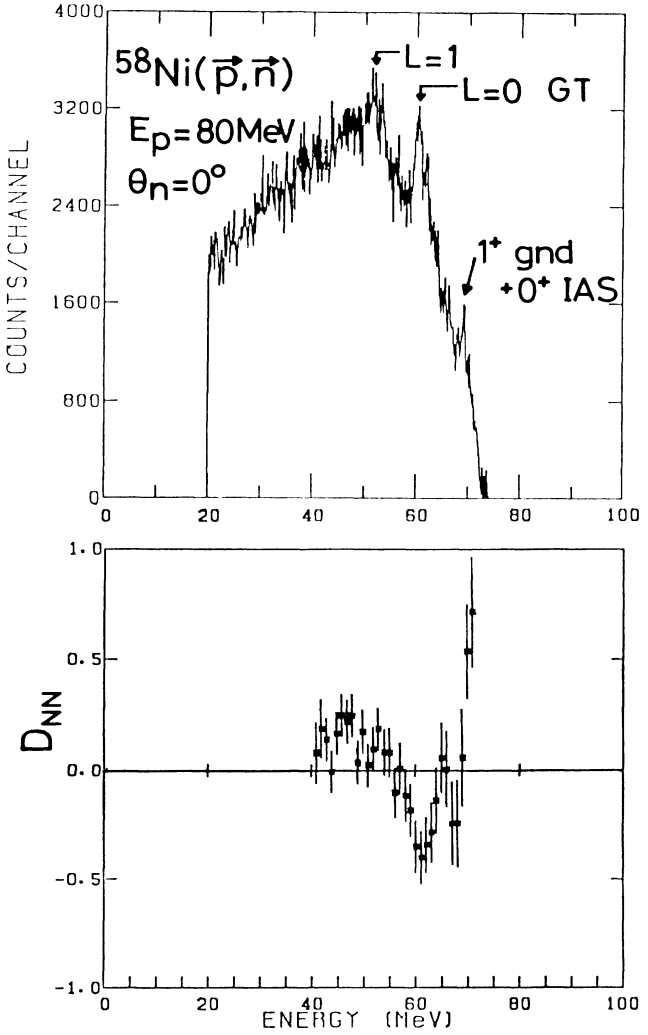

FIG. 2. Energy spectrum (upper) and transverse polarization transfer $D_{NN}(0°)$ (lower) for the ^{58}Ni(p,n) reaction at $\theta=0°$ and $E_p=80$ MeV. The normalization uncertainty is about 10% in the lower spectrum.

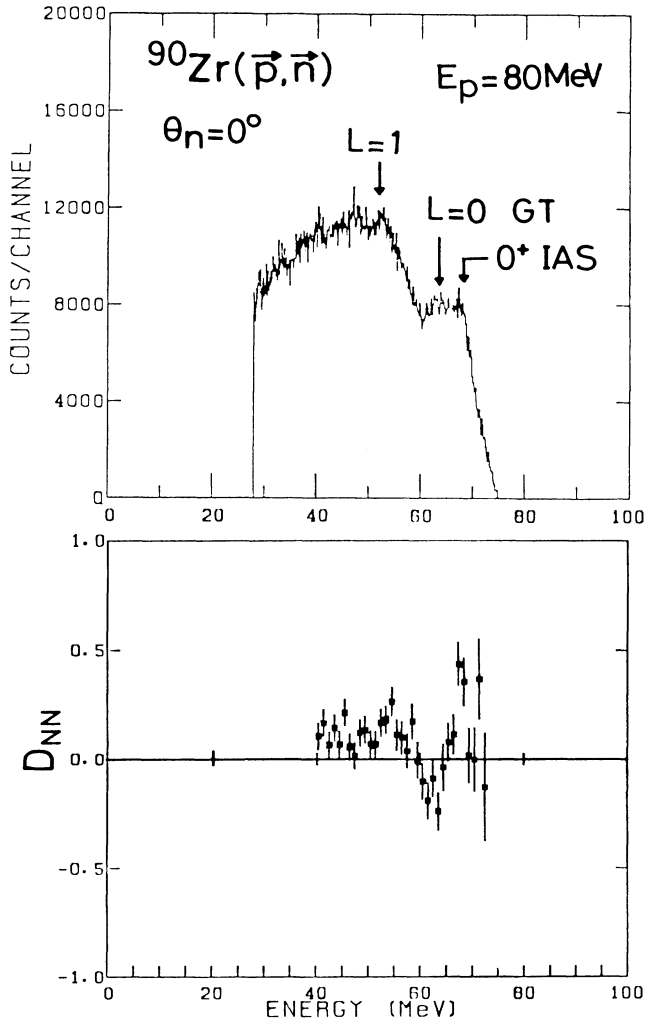

FIG. 3. Same as Fig. 2, but for the ^{90}Zr(p,n) reaction.

$\Delta S=1$ transitions. The dipole resonance region shows small positive values, indicating the mixture of $\Delta S=0$ and 1 transitions.

Spectra of the spin-flip cross section σS_{NN} and the non-spin-flip cross section $\sigma(1-S_{NN})$ for the ^{58}Ni and ^{90}Zr targets are shown in Figs. 4 and 5, respectively. It is interesting to see that the IAS peak stands out clearly in the $\sigma(1-S_{NN})$ spectrum, while the GT peak stands out in the σS_{NN} spectrum. The feature of the dipole resonance region is even more interesting. The peak, particularly in ^{90}Zr, stands out in the $\sigma(1-S_{NN})$ spectrum, indicating the predominance of the non-spin-flip dipole strength; in contrast, essentially no peak is seen in the σS_{NN} spectrum. This fact is in good agreement with the general trends of theoretical expectations.[11] The width of the non-spin-flip dipole resonance is consistent with that observed in the ^{89}Y,^{90}Zr(γ,n) reaction.[12]

V. COMPARISON WITH PWIA

In this section we will try to account for the observed $D_{NN}(0°)$ in terms of a simple plane wave impulse approximation (PWIA), as described in Sec. III. Comparisons are made only for the D_{NN} values of the ^{58}Ni(p,n)^{58}Cu reaction, since the detailed spectroscopic information required is available in the literature.[9]

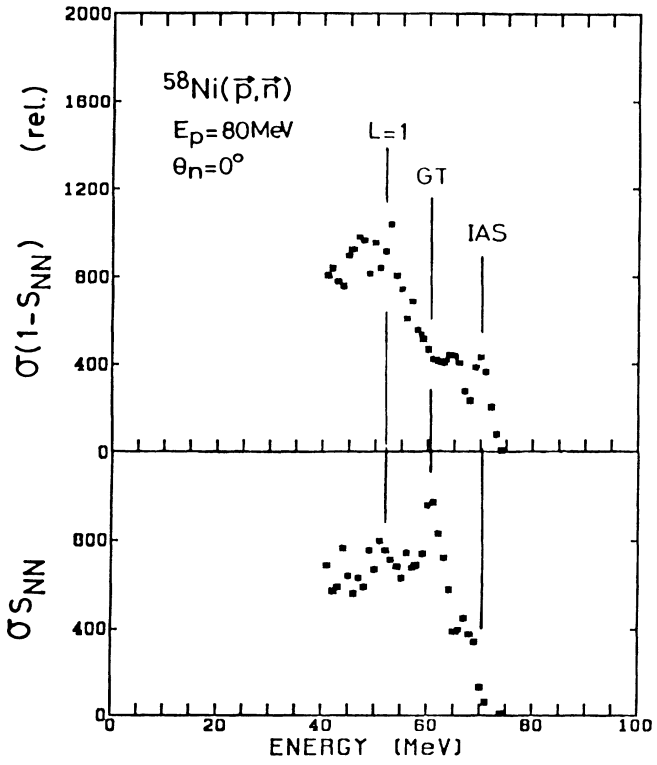

FIG. 4. The spin-flip (lower) and non-spin-flip cross sections (upper) for the ^{58}Ni(p,n) reaction at $\theta=0°$ and $E_p=80$ MeV.

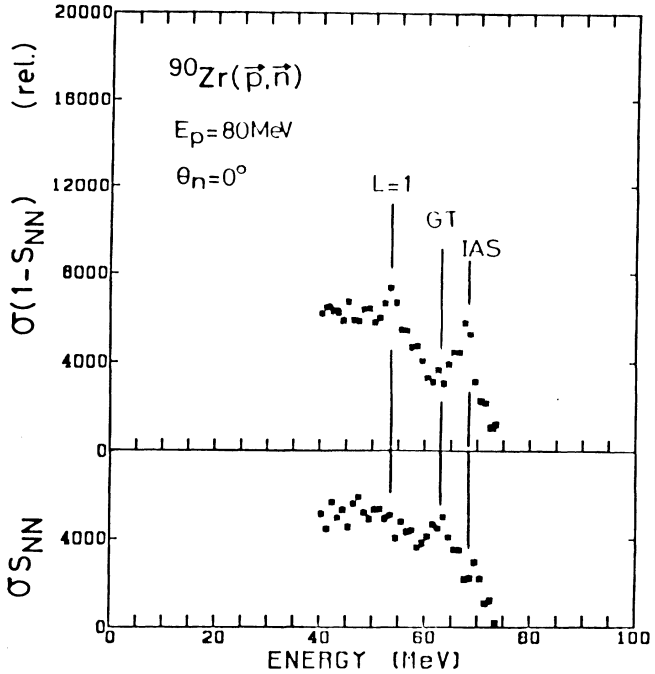

FIG. 5. Same as Fig. 4, but for the ^{90}Zr(p,n) reaction.

A. IAS region

The observed D_{NN} near the IAS region is a mixture of the Fermi (F) transition of IAS at $E_x=0.203$ MeV, GT transitions to the ground state, and a state at $E_x=1.052$ MeV. The Fermi strength $B(F)$ for the IAS is 2.0, and the sum strength for the GT transitions B(GT) is 0.57.[9] The energy dependence of the ratio (spin flip to non-spin-flip),

$$[R(E_p)]^2=\frac{\sigma_{GT}(0°)/B(GT)}{\sigma_F(0°)/B(F)}\frac{K_F(E_p)}{K_{GT}(E_p)}\ , \tag{12}$$

has been determined empirically by Taddeucci *et al.*[13] as

$$R(E_p)=E_p(\text{MeV})/55\ . \tag{13}$$

Here the kinematic factors are almost equal, $K_{GT}\approx K_F$. Thus the cross section ratio can be estimated as

$$\frac{\sigma_{GT}(0°)}{\sigma_F(0°)}=0.64\ .$$

From Eq. (11), the Fermi transition ($\Delta L=0$, $\Delta S=0$) gives $D_{NN}(0°)=1$, while the GT transition ($\Delta L=0$, $\Delta S=1$) gives $D_{NN}(0°)=-\frac{1}{3}$. Thus we can estimate the $D_{NN}(0°)$ for the IAS region as

$$D_{NN}(0°)=\frac{\sigma_{GT}(0°)\times(-\frac{1}{3})+\sigma_F(0°)\times 1}{\sigma_{GT}(0°)+\sigma_F(0°)}=0.48\ .$$

This value should be compared to the observed value 0.44 ± 0.13, showing excellent agreement.

B. Gamow-Teller giant resonance region

The GT giant resonance was observed as a peak at around $E_x=9$ MeV in ^{58}Cu. The observed value after

averaging over a 3 MeV width is

$$D_{NN}(0°) = -0.36 \pm 0.07$$

for the GT giant resonance (GTGR) region. Note again that this value is extracted without any background subtraction. This value is very close to the $-\frac{1}{3}$ expected for the pure GT transition by use of PWIA. In order to assess the distortion effect, distorted-wave Born approximation (DWBA) calculations including realistic effective interactions and knock-on exchange amplitudes have been performed. The effective interactions are those of M3Y.[14] The shell model wave functions which reproduce the spreading effect reasonably well are employed for the GT giant resonance $T=0$, 1, and 2 states.[15] The distorting potentials are taken from Ref. 16. These calculations show that D_{NN} appears to be sensitive to the tensor interaction and not to the distorting potentials. Note that the tensor interaction should enter mainly through the knock-on exchange interaction at $\theta=0°$. All calculated results have values of $D_{NN}(0°) = -0.40 \pm 0.05$. These values are slightly more negative than the observed value. If we assume the difference is solely due to non-spin-flip background ($D_{NN}=1.0$), then only a 4% background yield under the GT giant resonance peak is required to explain the observed difference. Thus our $D_{NN}(0°)$ data for the GT giant resonance region seem to indicate that most of the yield beneath the apparent GTGR peak is also due to transitions with $\Delta S=1$. A somewhat similar conclusion was obtained by Rapaport *et al.*[9] by using differential cross section data alone.

C. Dipole resonance region

A rather broad bump was observed in the energy spectrum at around $E_x=18$ MeV. The peak energy corresponds to that of the giant dipole resonance ($\Delta L=1$, $\Delta S=0$), as observed in the reaction ^{58}Ni(γ,n).[17] It is expected that a spin-flip dipole resonance ($\Delta L=1$, $\Delta S=1$) exists at about the same energy[18] and is considered to be a superposition of three components with $J^\pi=0^-$, 1^-, and 2^-. Our data show that $D_{NN}(0°)$ changes smoothly from negative values at the GT giant resonance to values of $+0.1$ to $+0.2$ at the $E_x=18$ MeV bump.

Table I shows $D_{NN}(0°)$ and the relative values of $d\sigma/d\Omega$ with $2J+1$ statistical factors. $\overline{D}_{NN}$ is the average coefficient weighted by the $J=0^-$, 1^-, and 2^- strengths. Some random-phase-approximation (RPA) calculations[11] have shown that the $J=1$ strength, and especially the $J=2$ strength, may be less efficiently localized by the residual interaction; weightings reflecting these calculations are given in parentheses. The $\overline{D}_{NN}$ values are changed only slightly by such a change in the weightings.

TABLE I. $D_{NN}(0°)$ predicted from the PWIA and the relative $d\sigma/d\Omega$ with $2J+1$ statistical factors. D_{NN} is the average $\overline{D}_{NN}$ weighted by $d\sigma/d\Omega$. Values in parentheses are those with different weightings.

	J^π	$D_{NN}(0°)$	Relative $d\sigma/d\Omega$	$\overline{D}_{NN}$
Non-spin-flip	1^-	1		1
Spin flip	0^-	-1	1 (1)	
	1^-	0	3 (2)	$-\frac{1}{3}$ $(-\frac{9}{25})$
	2^-	$-\frac{2}{5}$	5 (2)	

Now let us estimate the strength of the spin-flip dipole resonance by using the observed D_{NN} value, 0.14 ± 0.03, for $E_x=16$–26 MeV ($E_n=46$–55 MeV). From Table I we get

$$\frac{\sigma(\mathrm{NSF})\times 1+\sigma(\mathrm{SF})\times(-\frac{1}{3})}{\sigma(\mathrm{NSF})+\sigma(\mathrm{SF})}=0.14\pm0.03\ ;$$

therefore

$$\sigma(\mathrm{SF})/\sigma(\mathrm{NSF})=1.8\pm0.3\ .$$

Thus in the broad bump at around $E_x=18$ MeV the spin-flip dipole strength seems to be about 1.8 times stronger than the non-spin-flip dipole strength. Detailed comparisons of this result to theoretical predictions are not presently possible, because so far there have been no works published to our knowledge on the ^{58}Ni nucleus.

Summarizing, we have shown that the observed D_{NN} values of the IAS and GT giant resonance region are consistent with simple PWIA expectations. This fact may indicate that a simple PWIA prediction can be applied to reveal spin-flip and non-spin-flip strengths in unknown regions. Note that one must, however, bear in mind that spin-flip transitions are apt to give more or less similar D_{NN} values irrespective of the transferred angular momentum (see Table I).

Consequently, if the GT giant resonance overlaps with the spin-flip dipole resonance, then there is no way to distinguish one from the other by measuring $D_{NN}(0°)$ values. In such cases non-zero-degree data will certainly help to distinguish them.

VI. SPIN-FLIP AND NON-SPIN-FLIP STRENGTHS IN ^{90}Nb

Recently, experimental results for the $D_{NN}(0°)$ have been reported[19,20] for the ^{90}Zr(p,n) reaction at $E_p=120$ and 160 MeV. In this section we combine these higher energy results with our data to extract a strength ratio of spin-flip to non-spin-flip strength and the $D_{NN}(0°)$ value for the spin-flip transitions. These quantities are particularly interesting, since, for example, the experimentally obtained non-spin-flip strength in the GT giant resonance region may give important information on the continuum background under the resonance, which is crucial to extract a precise GT strength, and at the same time the D_{NN} value can be used to check for consistency with the transferred angular momentum ΔJ associated with spin flip.

Figure 6 shows the $D_{NN}(0°)$ values as a function of the excitation energy E_x for three different bombarding energies $E_p=80$, 120, and 160 MeV. The data at 80 MeV are the present results, and those at 120 and 160 MeV are the results of Taddeucci *et al.*[19,20] It is quite interesting to see the change of D_{NN} according to the bombarding energy.

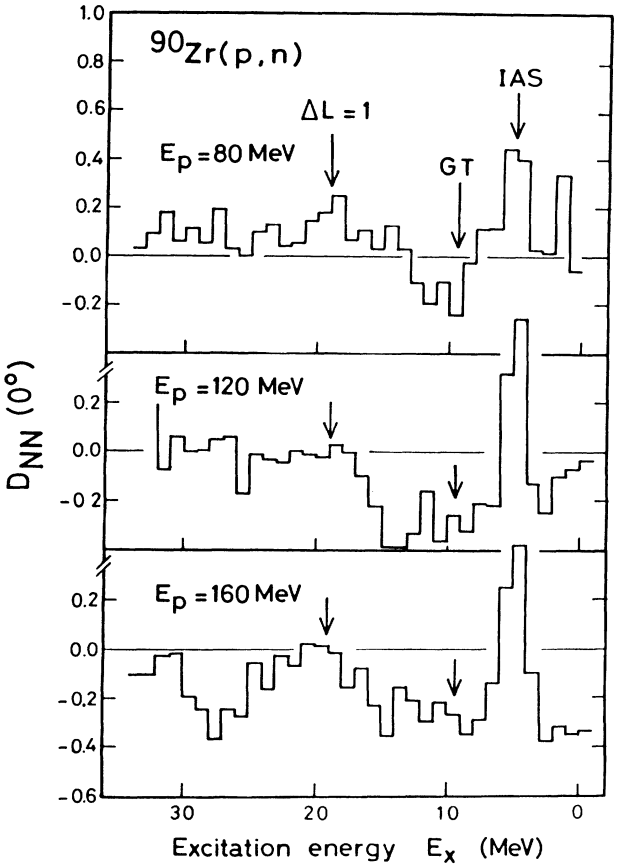

FIG. 6. The D_{NN} spectra as a function of excitation energy for the ^{90}Zr(p,n) reaction at $E_p=80$ 120, and 160 MeV. The data of 80 MeV are the present result; those of 120 and 160 MeV are taken from Tadeucci *et al.* (Ref. 19 and 20).

The D_{NN} value of the GT giant resonance region shows a very small E_p dependence. The D_{NN} of the dipole resonance region changes rather smoothly as a function of E_p from a positive value to a negative value, showing the change of the relative magnitudes of isovector spin-dependent and spin-independent interactions in the effective nucleon-nucleon force ($V_{\sigma\tau}/V_\tau$). The large negative dip observed at $E_x\simeq 28$ MeV in the 160 MeV spectrum is not observed in the 80 MeV spectrum or in the 120 MeV spectrum.

The strength ratio f of the non-spin-flip strength over the spin-flip strength and the D_{NN}(SF) for the spin-flip transition can be obtained by assuming the same energy dependence of the spin-flip strength over non-spin-flip strength ($V_{\sigma\tau}/V_\tau$) for all $\Delta L\neq 0$ transitions as that for $\Delta L=0$, i.e., $R(E_p)$. The experimentally observed transverse polarization transfer D_{NN}^{expt} is related to the spin-flip and non-spin-flip cross sections and D_{NN} as

$$D_{NN}^{\text{expt}}=\frac{\sigma(\text{SF})D_{\text{NN}}(\text{SF})+\sigma(\text{NSF})D_{\text{NN}}(\text{NSF})}{\sigma(\text{SF})+\sigma(\text{NSF})}\ , \tag{14}$$

where D_{NN}(SF) [D_{NN}(NSF)] is the polarization transfer for the spin-flip (non-spin-flip) transitions, and σ(SF) [σ(NSF)] is the spin-flip (non-spin-flip) cross section. According to Eq. (12),

$$[R(E_p)]^2=\frac{\sigma(\text{SF})}{\sigma(\text{NSF})}\frac{S(\text{NSF})}{S(\text{SF})}\ , \tag{15}$$

where S(SF) [S(NSF)] is the spin-flip (non-spin-flip) nuclear structure factor. At momentum transfer $q=0$ and angular momentum transfer $\Delta L=0$, S(SF) [S(NSF)] becomes the reduced transition probability[21] B(GT) [$B(F)$] for the analogous Gamow-Teller (Fermi) β-decay transition as given in Eq. (12). We define the strength ratio f as

$$f=\frac{S(\text{NSF})}{S(\text{SF})}\ . \tag{16}$$

Inserting Eq. (13) and (14) into Eq. (12), we get

$$D_{NN}(\text{SF})=\frac{D_{NN}^{\text{expt}}-D_{NN}(\text{NSF})}{[R(E_p)]^2}f+D_{NN}^{\text{expt}}\ . \tag{17}$$

We assume D_{NN}(NSF)=1.0. Equation (17) gives the relation between D_{NN}(SF) and f that we want to extract.

In the preceding section a D_{NN} value for the spin-flip transitions [$D_{NN}=-\frac{1}{3}$ for the GT giant resonance and $D_{NN}=-\frac{1}{3}$ for the dipole resonance (Table I)] has to be assumed *a priori* to extract the strength ratio of spin flip to non-spin-flip. A merit of the method in this section is that a D_{NN}(SF) value can be extracted directly from the experimental data in addition to the strength ratio f.

In Fig. 7 the D_{NN}(SF) are plotted as a function of f for

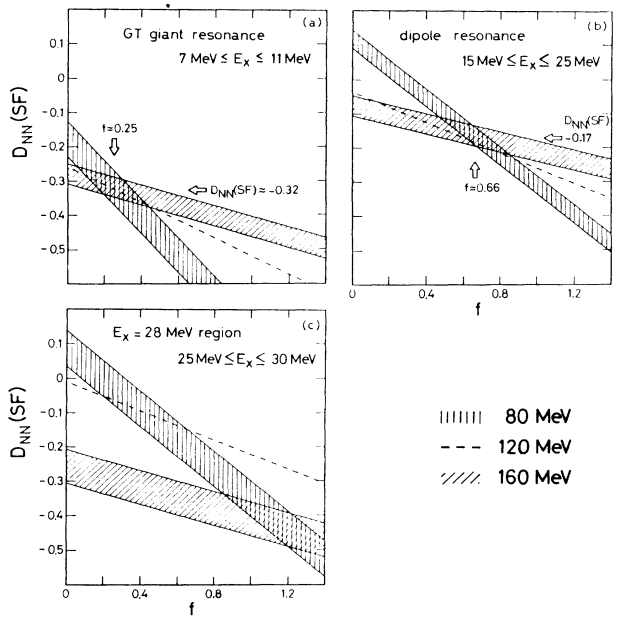

FIG. 7. Relation between D_{NN}(SF) and f plotted for three different projectile energies, $E_p=80$, 120, and 160 MeV. D_{NN}(SF) is the polarization transfer for the spin-flip transition and f is the ratio of non-spin-flip to spin-flip strengths. $f=0$ indicates no non-spin-flip strength. The crossing point determines a unique set of D_{NN}(SF) and f under the assumption of the energy dependence of $R(E_p)$ for the spin-flip to non-spin-flip strengths. Panel (a) is for the GT giant resonance region. Panel (b) is for the dipole resonance region. Panel (c) is for the $E_x=28$ MeV region. See text for further details.

three bombarding energies. The errors of the D_{NN}^{expt} for $E_p=120$ MeV have not been given in Ref. 20. The D_{NN}^{expt} values are obtained for the intervals $7\leq E_x\leq 11$ MeV, $15<E_x\leq 25$ MeV, and $25<E_x<30$ MeV, corresponding to the GT giant resonance, the dipole resonance, and the $E_x=28$ MeV regions, respectively. The D_{NN}^{expt} of the GT region for $E_p=80$ MeV is obtained as -0.18 ± 0.03 for the interval $9\leq E_x\leq 11$ MeV to avoid the contamination from the nearby IAS due to the poor energy resolution. Those of the dipole resonance and $E_x=28$ MeV regions are obtained as 0.11 ± 0.03 and 0.08 ± 0.05, respectively.

In Fig. 7 the slope is essentially determined by the factor $1/[R(E_p)]^2$. Thus the slope of $E_p=80$ MeV is about 4 times steeper than that of 160 MeV. This slope difference enables us to extract $D_{NN}(\text{SF})$ and f. The important role played by the 80 MeV data is clearly shown.

Figure 7(a) gives $D_{NN}(\text{SF})=-0.32\pm0.03$ and $f=0.25\pm0.10$ for the GT resonance region. The extracted $D_{NN}(\text{SF})$ is very close to the expected value $-\frac{1}{3}$ of PWIA for the GT transition. The f value can be used to estimate a possible non-spin-flip contamination in the GT giant resonance region. Inserting the obtained f value 0.25 to Eq. (15), one gets $\sigma(\text{NSF})/\sigma(\text{SF})=0.12\pm0.04$ and 0.03 ± 0.01 for 80 and 160 MeV, respectively. This result clearly indicates that the non-spin-flip background in the GT giant resonance region is indeed very small, particularly at 160 MeV. This fact may provide an important clue to subtracting the background in the GT giant resonance which is crucial to extracting the GT strength for the quenching phenomena.

At the dipole resonance region, $D_{NN}(\text{SF})=-0.17\pm0.03$ and $f=0.66\pm0.14$ can be deduced from Fig. 7(b). The large f value indicates the significant contributions from the non-spin-flip isovector giant dipole resonance, as expected.[11] The PWIA for the spin-flip dipole resonances $J^\pi=0^-,1^-,2^-$ gives rise to $D_{NN}\approx-\frac{1}{3}$ with simple cross section ratio weightings, as shown in Table I. The present result, -0.17 ± 0.03, may thus indicate that the relative strength of 1^- ($\Delta S=1$) state is about 3–4 times larger than that of the PWIA expectation in the interval $15<E_x\leq 25$ MeV. The less negative D_{NN} value can be explained only by the stronger 1^- strength, which has $D_{NN}=0.0$. The average excitation energies for $J^\pi=0^-$, 1^-, and 2^- states are estimated to be about 25, 21, and 16.5 MeV, respectively, but using the Hartree-Fock random-phase approximation by Klein and Love.[22] Therefore the present interval $15<E_x\leq 25$ MeV is most likely not wide enough to include all the 0^- and 2^- dipole components. This f value is also consistent with that estimated in the preceding section on ^{58}Ni, which gives $f=0.56\pm0.08$.

Figure 7(c) shows the $E_x=28$ MeV region. Here a good overlap region with three projectile energies no longer exists. The intersection between the 80 and 120 MeV data gives $D_{NN}(\text{SF})\sim-0.1$ and $f\sim0.4$, and that between 80 and 160 MeV data gives $D_{NN}(\text{SF})\sim-0.45$ and $f\sim1.2$. This large change of f may be explained if there is an unexpectedly large energy dependence in either or both the spin-flip and/or the non-spin-flip strengths. Some structure calculations[11,23] predict isovector monopoles (both non-spin-flip $J^\pi=0^+$, $\Delta S=0$, $D_{NN}=+1$, and spin flip $J^\pi=1^+$, $\Delta S=1$, $D_{NN}=-\frac{1}{3}$ are possible) as well as isovector quadrupoles ($J^\pi=1^+$, $\Delta S=1$, $\Delta L=2$) in this region. As for the isoscalar monopole resonance, an anomalous projectile energy dependence has been reported.[24] One may probably expect the same kind of phenomenon in the isovector monopole resonance as well. In any case, strengths which satisfy a strong projectile energy dependence and at the same time bear a large negative $D_{NN}(\text{SF})$ value, such as 0^- states ($D_{NN}=-1$), are needed to explain the large change of $D_{NN}(\text{SF})$.

It has been pointed out by Love and Klein[8] that D_{NN} quickly approaches zero beyond $q\geq0.5$ fm^{-1} due to the momentum transfer dependence of nucleon-nucleon interactions. The formulae of Eq. (11) are derived by assuming $q\simeq0$. The momentum transfer for $E_x=28$ MeV at 0° and $E_p=80$ MeV is about 0.5 fm^{-1}. Consequently, the energy dependence $[R(E_p)]$, which has been derived empirically[13] from the data with $q\leq0.2$ fm^{-1}, may be no longer applicable.

At this point it may be worth mentioning the possibility of contributions from multistep scattering processes. The multistep processes become important for lower incident energies and for large energy losses, i.e., large Q values. The observed D_{NN} values of $E_x=28$ MeV change sign, $D_{NN}\simeq+0.08$, 0.0, and -0.26 for $E_p=80$, 120, and 160 MeV, respectively. A naive picture of the multistep processes gives rise to $D_{NN}=0.0$. Therefore, contributions of the multistep processes result in the reduction of the D_{NN} values, and they cannot cause the experimentally observed sign change. Therefore it may be difficult to explain the characteristic features of D_{NN} values around $E_x=28$ MeV entirely by multistep processes.

Summarizing this section, $D_{NN}(\text{SF})$ and f are derived from the experimentally observed D_{NN} data at $E_p=80$, 120, and 160 MeV by assuming the empirically determined energy dependence $R(E_p)$. The deduced $D_{NN}(\text{SF})$ and f are consistent with PWIA predictions for the GT giant resonance and the dipole resonance regions. Some possible explanations are suggested for the unexpected projectile energy dependence of the $E_x=28$ MeV region.

VII. SUMMARY

We have measured the transverse polarization transfer coefficients D_{NN} for the (p,n) reaction on ^{58}Ni and ^{90}Zr targets at $\theta=0°$ and $E_p=80$ MeV. The observed D_{NN}'s for both targets show a quite similar pattern: large positive D_{NN} values in the IAS region, negative D_{NN} values in the GT giant resonance region, and small positive D_{NN} values at the dipole resonance and even higher excitation region. The D_{NN} values are interpreted in terms of the plane-wave impulse approximation (PWIA). For the ^{58}Ni target, we have shown that the GT giant resonance region seems to contain only 4% non-spin-flip background, and the dipole resonance region is a mixture of spin-flip type ($J^\pi=0^-,1^-,2^-$) transitions and a non-spin-flip ($J^\pi=1^-$) transition. The spin-flip dipole cross section seems to be about 1.8 times larger than the non-spin-flip cross section.

For the ^{90}Zr target, we have deduced the value of D_{NN}(SF) for the spin-flip transitions and the ratio f of the non-spin-flip strength to the spin-flip strength directly from experimental data at three different bombarding energies. The D_{NN} data at 80 MeV are the present result and those at 120 and 160 MeV are the results by Taddeucci *et al.*[19,20] Here the energy dependence $R(E_p)$ (Ref. 13) of the spin-flip strength to the non-spin-flip strength has been assumed irrespective of the transferred angular momentum. The derived D_{NN}(SF) value for the GT region, -0.32 ± 0.03, is in good agreement with the PWIA prediction. The non-spin-flip backgrounds at the GT giant resonance region, which are very important in extracting the GT strength related to the quenching phenomenon, are obtained as $\sigma(\text{NSF})/\sigma(\text{SF})=0.12\pm0.04$ and 0.03 ± 0.01 at $E_p=80$ and 160 MeV, respectively, indicating a very small value at higher incident energy. In the dipole resonance region $15<E_x\leq25$ MeV the obtained D_{NN}(SF) was -0.17 ± 0.03, indicating a strong concentration of the spin-flip dipole component of $J^\pi=1^-$ states compared to other spin-flip dipole $J^\pi=0^-$ and 2^- components, which is theoretically expected.[11,23] At the highly excited region $E_x\approx28$ MeV, we could derive neither D_{NN}(SF) nor f due to the strong bombarding energy dependence of observed D_{NN} values, and we have discussed some possible explanations. We would like to stress the importance of our low energy data, which played an essential role in determining the D_{NN}(SF) and f by virtue of the higher sensitivity to non-spin-flip strengths.

ACKNOWLEDGMENTS

We thank Toru Suzuki for valuable discussions and also K. Mutoh for providing us shell model wave functions. One of us (H. S.) would like to thank J. M. Moss for his hospitality at Los Alamos National Laboratory, where part of analysis was performed. We are grateful to Dr. D. Hinde for reading the manuscript. We appreciate the support and encouragement of H. Ikegami and M. Kondo for this work. This work was supported in part by a Grant-in-Aid for Scientific Research, No. 58540156, of the Japan Ministry of Education, Science and Culture. This experiment was performed at the Research Center for Nuclear Physics under Program Nos. 18A08 and 20A25.

*Present address: National Laboratory for High Energy Physics (KEK), Oho, Tsukuba, Ibaraki 305, Japan.

[1]C. D. Goodman and S. D. Bloom, in *Spin Excitations in Nuclei,* edited by F. Petrovich *et al.* (Plenum, New York, 1984).
[2]J. M. Moss, Phys. Rev. C **26**, 727 (1982).
[3]H. Sakai, M. Ieiri, K, Imai, N. Matsuoka, T. Motobayashi, T. Saito, A. Sakaguchi, and A. Shimizu, in *Antinucleon- and Nucleon-Nucleus Interactions,* edited by G. E. Walker, C. D. Goodman, and C. Olmer (Plenum, New York, 1985), p. 293.
[4]H. Sakai, N. Matsuoka, T. Noro, T. Saito, and A. Sakaguchi, Nucl. Instrum. Methods A **244**, 449 (1986).
[5]Madison Convention: in *Proceedings of the Third International Symposium on Polarization Phenomena in Nuclear Reactions,* Madison, 1970, edited by H. H. Barschall and W. Haeberli (University of Wisconsin Press, Madison, 1971).
[6]H. Sakai, N. Matsuoka, T. Noro, T. Saito, A. Shimizu, M. Tosaki, M. Ieiri, K. Imai, A. Sakaguchi, Y. Takeuchi, and T. Motobayashi, Nucl. Instrum. Methods (to be published).
[7]A. K. Kerman, H. McManus, and R. M. Thaler, Ann. Phys. (N.Y.) **8**, 551 (1959).
[8]W. G. Love and Amir Klein, J. Phys. Soc. Jpn. Suppl. **55**, 78 (1986).
[9]J. Rapaport, T. N. Taddeucci, T. P. Welch, C. Gaarde, J. Larsen, D. J. Horen, E. Sugerbaker, P. Koncz, C. C. Foster, C. D. Goodman, C. A. Goulding, and T. Masterson, Nucl. Phys. A **410**, 371 (1983).
[10]D. E. Bainum, J. Rapaport, C. D. Goodman, D. J. Horen, C. C. Foster, M. B. Greenfield, and C. A. Goulding, Phys. Rev. Lett. **44**, 1751 (1980).
[11]For example, Toru Suzuki, in *Progress in Particle and Nuclear Physics,* edited by D. H. Wilkinson (Pergamon, Oxford, 1984), Vol. 11, p. 597.
[12]A. Lepretre, H. Beil, R. Bergere, P. Carlos, A. Veyssiere, and M. Sugawara, Nucl. Phys. A **175**, 609 (1971).
[13]T. N. Taddeucci, J. Rapaport, D. E. Bainum, C. D. Goodman, C. C. Foster, C. Gaarde, J. Larsen, C. A. Goulding, D. J. Horen, T. Masterson, and E. Sugarbaker, Phys. Rev. C **25**, 1094 (1981).
[14]G. J. Bertsch, J. Borysowicz, H. McManus, and W. G. Love, Nucl. Phys. A **284**, 399 (1977).
[15]K. Mutoh, private communication.
[16]P. Schwant, H. O. Meyer, W. W. Jacobs, A. D. Bacher, S. E. Vigdor, M. D. Kaitcuck, and T. R. Donoghue, Phys. Rev. C **26**, 55 (1982).
[17]S. C. Fulz, R. A. Alvarez, B. L. Berman, and P. Meyer, Phys. Rev. C **10**, 608 (1974).
[18]C. Gaarde, J. Rapaport, T. N. Taddeucci, C. D. Goodman, C. C. Foster, B. E. Bainum, C. A. Goulding, H. B. Greenfield, D. J. Horen, and E. Sugarbaker, Nucl. Phys. A **369**, 258 (1981).
[19]T. N. Taddeucci, C. D. Goodman, R. C. Byrd, I. J. van Heerden, T. A. Carey, D. J. Horen, J. S. Larsen, C. Gaarde, J. Rapaport, T. P. Welch, and E. Sugarbaker, Phys. Rev. C **33**, 746 (1986).
[20]T. N. Taddeucci, J. Phys. Soc. Jpn. Suppl. **55**, 151 (1986).
[21]A. Bohr and B. R. Mottelson, *Nuclear Structure* (Benjamin, New York, 1969), Vol. 1, p. 345.
[22]Amir Klein and W. G. Love, Phys. Rev. C **33**, 1920 (1986).
[23]N. Auerbach and Amir Klein, Nucl. Phys. A **395**, 77 (1983).
[24]T. Yamagata, S. Kishimoto, K. Yuasa, B. Saeki, K. Iwamoto, M. Tanaka, T. Fukuda, I. Miura, M. Inoue, and H. Ogata, Nucl. Phys. A **381**, 277 (1982).